MICROSTRUCTURAL CHARACTERIZATION OF Ti-20Nb ALLOY FOR ORTHOPEDIC IMPLANTS

Giorgia Taiacol Aleixo
UNICAMP/FEM/DEMA - CP 6122, CEP 13087-970, Campinas SP - Brazil
giorgia@fem.unicamp.br

Camila Scaranelo
UNICAMP/FEM/DEMA - CP 6122, CEP 13087-970, Campinas SP - Brazil
camila@dep.fem.unicamp.br

Conrado Ramos Moreira Afonso
UNICAMP/FEM/DEMA - CP 6122, CEP 13087-970, Campinas SP - Brazil
croma@fem.unicamp.br

Rubens Caram
UNICAMP/FEM/DEMA - CP 6122, CEP 13087-970, Campinas SP - Brazil
rcaram@fem.unicamp.br

Abstract. *Beta titanium alloys form one of the most versatile classes of materials with respect to processing, microstructure and mechanical properties, mainly applications regarding biomaterials. Development of new Ti-based alloys for implant application involves more biocompatible metallic alloying elements, such as Nb, Ta, Zr and Mo. The aim of this work is the analysis of microstructure and phases formed during water quenching of β Ti-20Nb alloy through different cooling rates. Ti-20Nb alloy was sawged at 780-860ºC and then machined as a cylinder. Cylindrical sample was treated in β field and then water quenched from the bottom imposing different cooling rates through the sample. Samples from different regions (cooling rates) were characterized by using X-ray diffractometry (XRD), scanning (SEM) and transmission electron microscopy (TEM). Vickers microhardness was measured with a load of 200 gf. XRD shows that ratio between intensities of β and α" phases increases with decreasing of cooling rate. As the distance from the bottom (quenching water) of Ti-20Nb sample decreases, the cooling rate imposed increases, the volume of α" martensite acicular phase increases and the size decreases together with diminishing of α phase quantity.*

Keywords*: Beta Ti Alloy, Microstructural Characterization, Metastability, Cooling Rate.*

1. Introduction

Beta titanium alloys form one of the most versatile classes of materials with respect to processing, microstructure and mechanical properties. These alloys include β, metastable β and beta-rich α+β alloys and they can be found in aerospace, power plant, sporting goods, automotive, orthodontic and orthopedic implants applications (Weiss, 1998; Lütjering, 1998). Table 1 shows some of the advantages and disadvantages of beta alloys when compared to α+β alloys (Leyens, 2003). Increased use of titanium alloys as biomaterials is occurring due to their reduced elastic modulus, superior biocompatibility, strength-weight ratio, enhanced corrosion resistance, superior strain-controlled and notch fatigue resistance when compared to more conventional stainless steel and Co-Cr alloys (Long, 1998). Ti-6Al-4V, the most common titanium alloy is a good material for surgically implanted parts, such as knees, hips and shoulder replacement (Lee, 2003; Ramirez, 2003). However, the element V has been found to react severely with tissue in animals. Also, the use of Al is of concern because it may be connected to neurological disorders and Alzheimer's disease (Silva, 2004). Hence, recent works from Hon *et al.* (2003) and Zhou *et al.* (2004) showed that the synthesis of new Ti-based alloys for implant application involves more biocompatible metallic alloying elements, such as Nb, Ta, Zr and Mo (Niinomi, 2002). One of the keys for successful application of beta alloys is the development of appropriate processing conditions. Systematic correlations between processing, microstructure and properties must be derived in order to find a technically reasonable and safe processing window (Leyens, 2003).

Long-term studies indicate that insufficient load transfer from artificial implant to adjacent remodeling bone may result in bone resorption and eventual loosening of the prosthetic device (Azevedo, 2002). This phenomenon, termed "stress shielding effect", is direct result of the stiffness mismatch between implant materials and surrounding natural bone (Hon, 2003). Finite element analysis suggested that a lower modulus hip prosthesis better assimilates the natural femur in distributing stress to the adjacent bone tissue. Animal study also suggested that bone remodeling commonly experienced by hip prosthesis patients may be reduced by a prosthesis having a lower modulus (Lee, 2002). In this way, one of the goals of studying β-type Ti alloys is the diminishing of elastic modulus, because the common alloys used as biomaterials present too high values (4-7 times higher) when compared to that of the human bone (30 GPa), such as Ti-6V-4Al (108 GPa), 316 L stainless steel (200 GPa) or Co-Cr-Mo (210 GPa) alloys (Lütjering, 2003). Recently,

developed biocompatible Ti-based alloys have a trend of including relatively large amounts of beta stabilizer elements such as Nb, Zr and Ta (Kobayashi, 2002; Li, 2002; Hon, 2003; Lee, 2003; Zhou, 2004; Silva, 2004). Regarding the elastic modulus, it was reported by Hon *et al.* (2003) that a Nb content in the range of 10-20 mass% or in the range of 35-50 mass% favors attaining a relatively low value of 60 GPa. Deviations from the ranges mentioned above lead to an increase in the elastic modulus.

Table 1. Advantages and disadvantages of β alloys when compared to α+β titanium alloys (Leyens, 2003).

Advantages	Disadvantages
- high strength-to-density ratio - low elastic modulus - high strength/high toughness - good deep hardenability - low forging temperature - strip producible – low cost TMP * (some alloys) - cold formable (some alloys) - easy to heat treat - excellent corrosion resistance (some alloys) - excellent combustion resistance (some alloys)	- high density - low elastic modulus - poor low and high temperature properties - high formulation cost - segregation problems - high spring back - microstructural instabilities - poor corrosion resistance (some alloys) - interstitial pick up

* TMP: thermomechanical processing

According to the equilibrium phase diagram of binary Ti-Nb system a Ti-20Nb alloy under cooling from solution heat treatment at β field can show a microstructure that depends on the cooling rate imposed to the sample as well as the temperature used for the heat treatment and the end of cooling. For this composition, under furnace cooling, the microstructure is constituted essentially of α + β. When the cooling rate imposed to the sample is high the microstructure changes from the previously described to a combination of β phase and martensite (α' or α"). As shown in qualitative diagram represented in Figure 1, the alloy composition is fundamental in the constitution of final microstructure. For alloys with low solute β–stabilizer element content, the microstructure presents hexagonal structures typical of α phase or eventually α' martensite phase. For high solute β–stabilizer element content (α+β composition range) the type of martensite formed is orthorhombic martensite α".

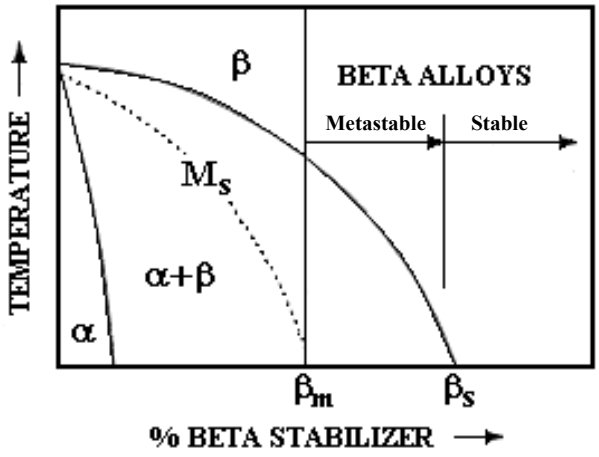

Figure 1. Pseudo-binary phase diagram of titanium alloys with β–stabilizer elements (Long, 1998).

Increasing even more the solute β–stabilizer content (near β composition range), under high cooling rates from the β field until room temperature is possible the obtaining of metastable or even stable β phase. Furthermore, depending on the composition, phase ω can be dispersed into the β matrix, turning the structure of material fragile. Metastable ω phase can be obtained directly from the cooling from the β field, being classified as athermal, or from the cooling from the β field until a intermediate temperature over M_s and then heat treated isothermally for a long time, causing the precipitation of isothermal ω phase. The aim of this work is the analysis of microstructure and phases formed during water quenching of β Ti-20Nb alloy through different cooling rates. The variation of cooling rate could lead to different microstructures and consequently different mechanical properties searching for a suitable combination applicable to biomaterials such as orthopedic implants.

2. Experimental Procedure

The binary Ti-20Nb alloy was prepared from high purity Ti sheets (99.84 %) and Nb pieces (99.99 %) according to nominal composition in an arc-melting furnace under vacuum and argon atmosphere. Ti-20Nb alloy was hot-forged by swaging at 780-860 ºC producing a final 11mm diameter rod and machined as a cylinder of 10.5 mm ∅ x 100 mm length. Cylindrical sample was submitted to solution treatment in β field (1000ºC/10min) and then water quenched from the bottom of the sample. Thermocouples were positioned at six different regions distant 5 mm each other, being the sixth thermocouple 1 mm from the surface in contact with the circulating water, similar to a Jominy End Quench Test. Figure 2 shows a schematic illustration of the experimental apparatus for water quenching of Ti-20Nb cylindrical sample. Samples from regions I to VI were characterized by using X-ray diffractometry (XRD) Rigaku DMAX 2200 using Cu-Kα radiation source. The specimens for the SEM analysis were mechanically grinded using SiC sandpaper up to 1200 mesh, polished with 6 and 1 μm diamond paste with ethylic alcohol as lubricant and then etched in a Kroll´s solution consisting of 5 vol%HF, 30 vol%HNO_3 and 65 vol%H_2O. The microstructures were observed in a scanning electron microscope (SEM) Jeol JXA 840A and transmission electron microscopy (TEM) was used to analyze the microstructures through a HRTEM - JEM 3010 URP equipment**.** Vickers microhardness was measured through a Buehler equipment, with a load of 200 gf applied for 15 s.

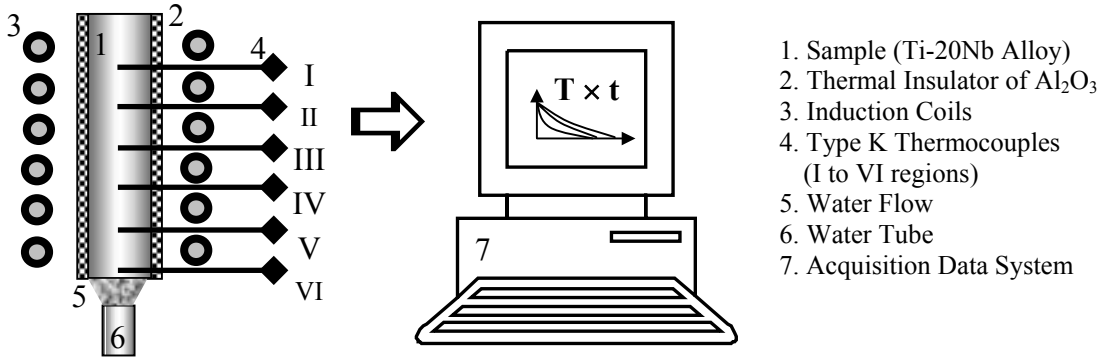

Figure 2. Schematic illustration of experimental apparatus for water quenching of Ti-20Nb cylindrical sample.

3. Results and Discussion

Optical micrographs of Ti-20Nb alloy hot-forged by swaging at 780-860 ºC and solution heat treated at 1000 ºC/8 h and furnace cooled are presented in Figure 3. Sample was submitted to this heat treatment condition in order to compare microstructure of slowly cooled sample with the ones of the proposed experiment. Figure 3.a shows general microstructure that is composed by α+β phases. Microstructure is formed by α phase dispersed in a β matrix, with α parallel plates growing from the α phase precipitated as a continuous layer along β grains boundaries. Figure 3.b shows higher magnification in detail of previous microstructure.

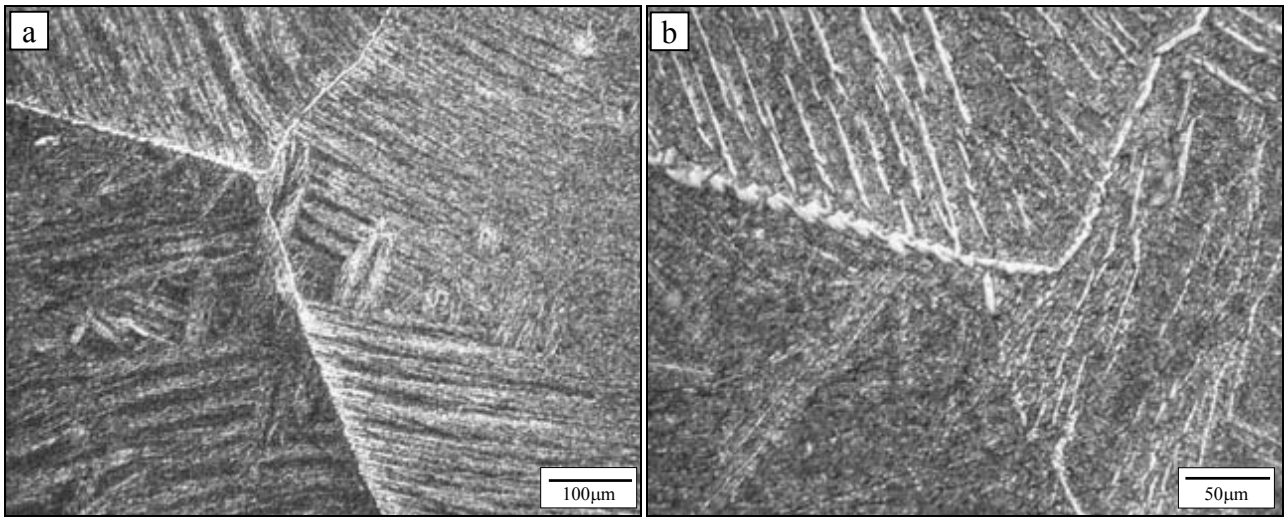

Figure 3. Optical micrographs showing the α phase dispersed in a β matrix of hot-forged and solution heat treated at 1000ºC/8h and furnace cooled Ti-20Nb sample.

Another cylindrical sample was hot-forged by swaging at 780-860 ºC and then submitted to solution treatment in β field and then water quenched from the bottom of the sample. Figure 4 presents the different thermal profiles of each thermocouple positioned along the cylindrical sample and cooling rates were determined for each region as illustrated in graphic of Figure 4.

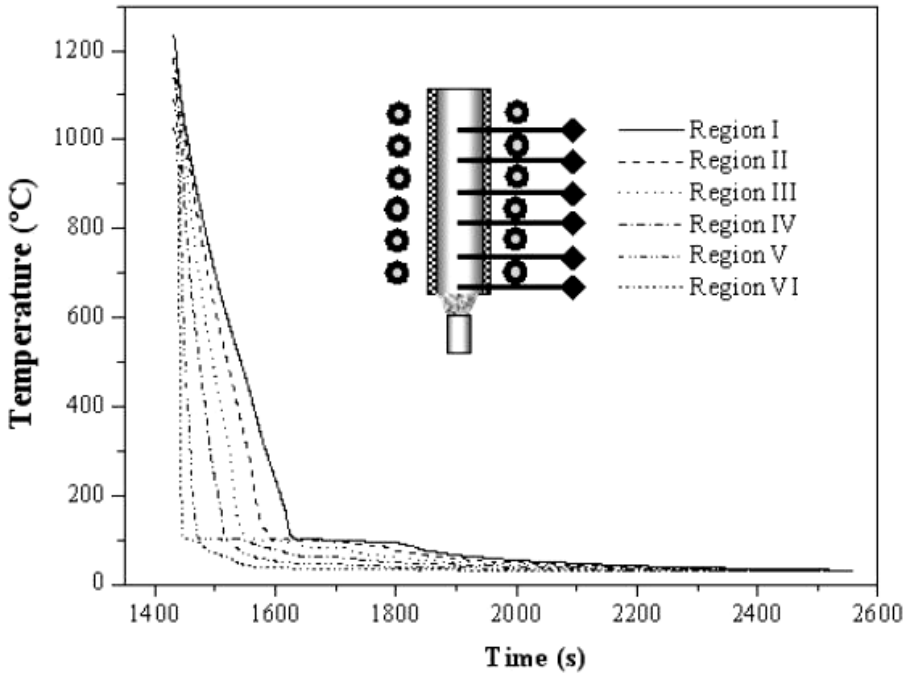

Figure 4: Thermal profiles of each thermocouple positioned along the cylindrical sample of Ti-20Nb alloy.

Cooling rates were determined in the temperature range from about 680 ºC, which is the β-*transus* temperature for Ti-20Nb alloy according to the Ti-Nb equilibrium diagram, down to 400 ºC. Under this temperature it is considered that the atomic diffusion is relatively not significant. Cooling rates between regions I and IV did not show expressive difference ranging from 4.6 to 11.5 K/s. Only from region IV to VI can be observed a significant variation of the cooling rates values of 11.5 to 139.6 K/s, respectively. Table 2 shows data of cooling rates (K/s) imposed to the cylindrical sample in different regions.

Table 2. Cooling rates (K/s) imposed to the cylindrical sample in different distances form the cooling water source.

Region	I	II	III	IV	V	VI
Cooling Rate (K/s)	4.6	6.0	7.9	11.5	27.3	139.6

Figure 5.a presents X-ray diffractograms of Ti-20Nb alloy quenched through different cooling rates (Regions I to VI), like illustrated in Fig. 1 and Fig. 4, where phases formed varied according to the cooling rate imposed. Although cooling rates between regions I and IV did not vary much, it can not be identified a relationship between formation of ω phase and the variation of cooling rate by from region I to IV. As the cooling rate increases (from region I to VI), the volume fraction of α" phase increases with the diminishing of fraction of α phase. This result is in agreement with the ones from the literature, in which the increasing of cooling rate in β-Ti alloys favors the formation of finer structures including the formation of martensite α" (Tang, 2000). It can be found a correlation between the diminishing of β phase fraction and the increasing of α" phase, due to the greater transformation of β phase fraction to α" martensite structure while cooling rate from region I to VI increases. Figure 5.b presents XRD diffractogram of region VI at lower scanning speed with more details and higher intensity peaks. Ratio between intensities of β and α phases increases with decreasing of cooling rate (Tang, 2000).

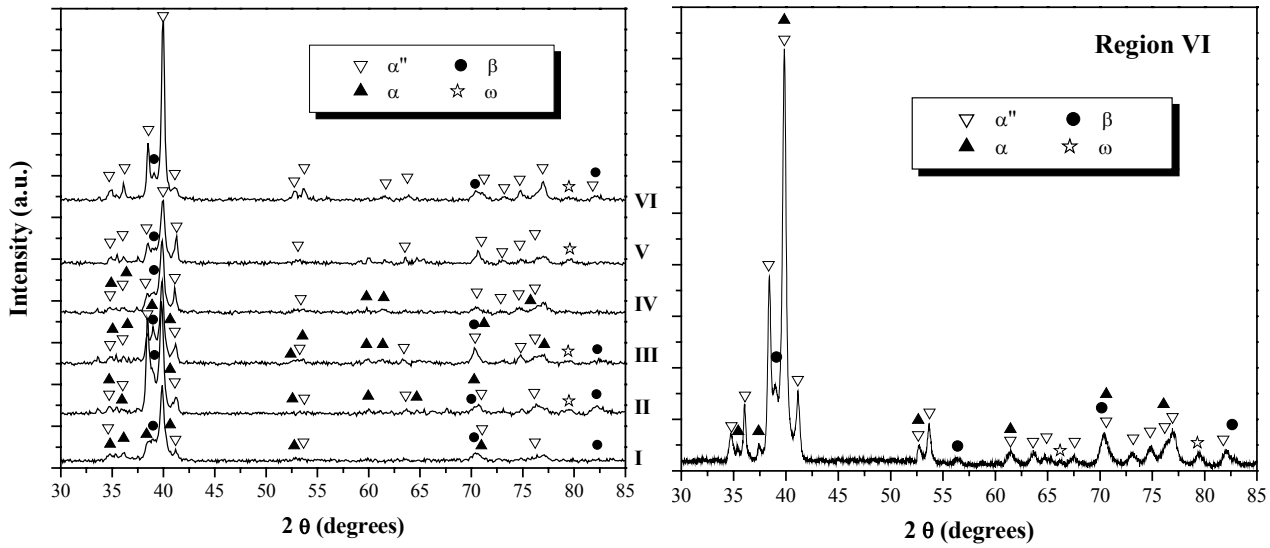

Figure 5. (a) X-ray diffractograms of Ti-20Nb alloy water quenched through different cooling rates (I to VI) and (b) diffraction pattern of region related with thermocouple VI in detail showing additional low intensity peaks.

Figure 6 shows SEM micrographs of Ti-20Nb alloy obtained through different cooling rates. Figures 6.a to 6.e show microstructures of samples in regions I to VI including phases α, α" and β varying in size and volume. According with the slightly variation of the cooling rate from region I to IV showed in Table 2, there is only a different microstructure when comparing region I with the others regions (II to IV). Fig 6.a shows microstructure of slower cooling rate (farther from the coolant water source) with a few quantity of α" martensite acicular phase dispersed in the β grains. Besides that it can be seen the precipitation of α phase along β grain boundaries resulting in a fine continuous layer. Similar microstructures from region II to VI are shown in Figs. 6.b to 6.d and the size of acicular α" martensite decreased and its volume increased when compared to Fig. 6.a (region I). As the cooling rate increases from region IV to VI the volume fraction of α" phase increases (together with size decreasing) with the diminishing of α continuous layer along β grain boundaries. This result is in agreement with the ones from the literature, in which the increasing of cooling rate in β-type Ti alloys favors the formation of finer structures including the formation of α" martensite (Tang, 2000). It can be found a correlation between the diminishing of β phase fraction and the increasing of α" phase, due to the greater transformation of β phase fraction to α" martensite structure while cooling rate from region I to VI increases.

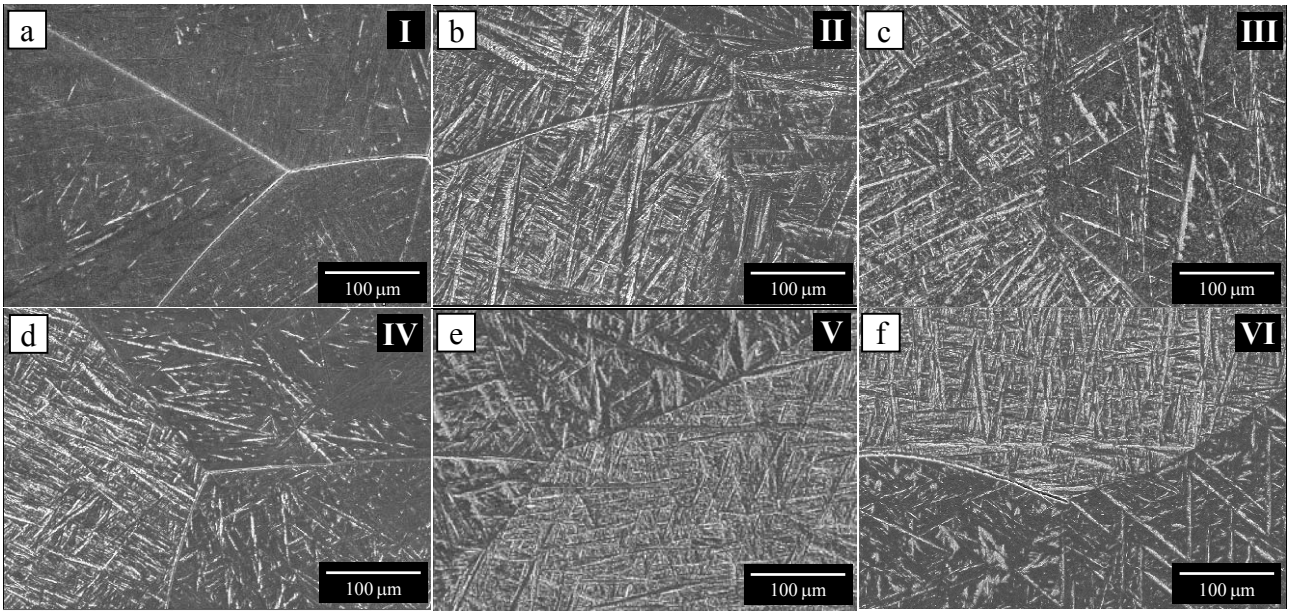

Figure 6. SEM micrographs of Ti-20Nb alloy samples showing α, α" acicular phases and β grains varying in size and volume according to the cooling rate imposed. From region I to VI as the cooling rate (K/s) increases, volume of α" martensite acicular phase increases and size decreases while size of β grains decreases.

TEM analysis of Ti-20Nb alloy samples is presented in Figure 7. It shows sample quenched under slower cooling at region I with bright field (BF) image showing α" acicular phase and β matrix and respective SAPD of β matrix region identifying ω phase together with β (Fig. 7.a). Microstructure of region VI (highest cooling rate) is presented in Fig. 7.b illustrating increasing of α" martensite quantity in relation with β phase and respective SAPD of α" martensite together with β phase. Presence of metastable ω phase distributed within β matrix was confirmed by TEM analysis (Kobayashi, 2002), but it could not be identified any relationship between formation of ω phase and the cooling rate imposed during quenching of sample from solution heat treated cylinder in β field.

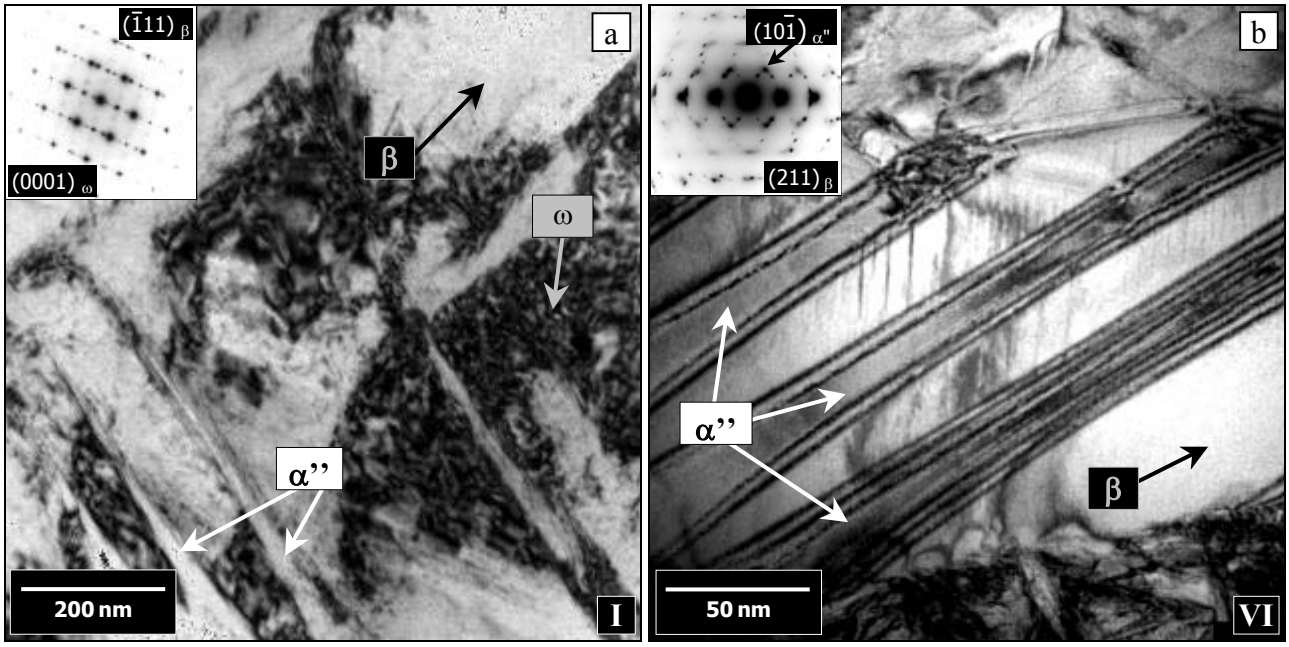

Figure 7. TEM analysis of Ti-20Nb alloy samples (a) quenched under slower cooling at region I with bright field (BF) image showing α" acicular phase and β matrix and respective SAPD of ω phase together with β phase. (b) Microstructure of region VI (highest cooling rate) showing increasing of α" martensite quantity in relation with β phase and SAPD of α" martensite together with β phase.

Evaluation of mechanical properties was measured through determination of Vickers microhardness with a load of 200 gf applied for 15 s. The values were determined based in different measurements of any given area through the sample. Table 3 shows cooling rates (K/s) imposed to the cylindrical sample, microhardness (HV) and respective phases identified in different distances form the cooling water source. It can be seen that there is a slightly increase of Vickers hardness with increasing of the cooling rate through the cylindrical sample, except from the value of region IV. It is coherent with the fact that increasing of cooling rate favors the martensite transformation of β phase to acicular α" provoking an increasing in the concentration of α" martensite distributed into the β grains.

Table 3. Cooling rates (K/s) imposed to the cylindrical sample, microhardness (HV) and respective phases identified in different distances form the cooling water source.

Results / Region	I	II	III	IV	V	VI
Cooling Rate (K/s)	4.6	6.0	7.9	11.5	27.3	139.6
Microhardness (HV)	221 ± 5	225 ± 9	226 ± 9	241 ± 15	237 ± 7	238 ± 10
Phases Formed	α, α", β	α, α", β	α, α", β	α, α", β	α", β	α", β

Phase identification through combination of SEM, XRD and TEM was satisfactory as well as Vickers microhardness measurements comparing with the results obtained by other authors (Lee, 2003; Hon, 2003) whom have studied Ti-Nb alloy ranging from 5–35wt%Nb and 14–40wt%Nb. Lee *et al.* (2003) processed Ti-20Nb in an arc-furnace, introducing a new system through quenching a cylinder in a graphite mold cavity at room temperature, obtaining a fully α" martensite microstructure. On the other hand, according to Hon *et al.* (2003) Ti-18Nb and Ti-22Nb alloys showed only α + β phases identified by XRD analysis when samples were hot rolled at 800ºC and solution heat treated at 700ºC (β field) for 3.6 ks and then furnace cooled to room temperature. Regarding mechanical properties, Lee *et al.* (2003) presented results of elastic modulus of about 60 GPa and Vickers microhardness of 280 HV and Hon *et al.* (2003) obtained an elastic modulus of 85 GPa.

According to figure 1 and microstructure of Ti-20Nb alloy (only α" martensite) obtained by Hon *et al.* (2003) it is clear that the composition studied can result in a completely β metastable state, depending on the cooling rate imposed. Considering that cooling routes adopted in previously described results were lower cooling rate trough furnace cooling by Lee *et al.* (2003) and higher cooling rate trough graphite mold casting by Hon *et al.* (2003), when compared with intermediary quenching condition used in the present work (water cooled through different cooling rates), the results obtained here are coherent. This is supported by (i) the values of Vickers microhardness obtained in the range of 220 to 240 HV that were smaller compared with 280 HV obtained through higher cooling rate condition and (ii) phase identification, which resulted in α, α" and β phases differs from α + β microstructure (α colonies precipitated along β grain boundaries) obtained through a lower cooling rate (furnace cooling) and α" martensite for the greater cooling rate. So, phases identified in the present study revealed a combination of both microstructures obtained in previously described extreme conditions.

4. Conclusions

The intensity ratio of α" and β peaks increases with the increasing of cooling rate. As the distance from the bottom (quenching water) of Ti-20Nb sample decreases, the cooling rate imposed increases, the volume of α" martensite acicular phase increases and the size decreases together with diminishing of α phase along β grain boundaries. Vickers microhardness increases with increasing of the cooling rate through the cylindrical sample and the increasing of α" martensite concentration into the β grains.

3. Acknowledgements

The authors would like to thank FAPESP, CAPES and CNPq for financial support and the researcher Antonio J. Ramirez from LNLS (National Laboratory of Synchrotron Light, Campinas, SP - Brazil) for the TEM analysis.

4. References

Azevedo, C.R.F. and Hippert Jr., E., 2002, "Failure Analysis of Surgical Implants in Brazil", Engineering Failure Analysis, Vol.9, pp. 621-633.

Hon, Y-H., Wang, J-Y. and Pan, Y-N., 2003, "Composition/Phase Structure and Properties of Titanium-Niobium Alloys, Materials Transactions", Materials Transactions, Vol.44, No. 11, pp. 2384-2390.

Lee, C.M., Ho, W.F., Ju, C.P. and Chern Lin, J.H, 2002, "Structure and Properties of Titanium-25Niobium-*x*Iron Alloys", Journal of Materials Science: Materials in Medicine, Vol.13, pp.695-700.

Lee, C.M., Ju, C.P. and Chern Lin, J.H, 2003, "Structure–Properties Relationship of Cast Ti-Nb Alloys", Journal of Oral Rehabilitation, Vol.29, pp.314-322.

Leyens, C. and Peters, M., 2003, "Titanium and Titanium Alloys – Fundamentals and Applications", DLR – German Aerospace Center – Institute of Materials Research, Wiley-VCH, Köln, Germany, 379 p.

Li, S., Hao, Y., Yang, R., Cui, Y. and Niinomi, M., 2002, "Effect of Nb on Microstructural Characteristics of Ti-Nb-Ta-Zr Alloy for Biomedical Applications", Materials Transactions, Vol.43, No.12, pp.2964-2969.

Long, M., Rack, H.J., 1998, "Titanium Alloys in Total Replacement – A Materials Science Perspective", Biomaterials, Vol.19, pp.1621-1639.

Lütjering, G. and Willians, J.C., 2003, "Titanium", Springer, Berlin, Germany, 513 p.

Niinomi, M., Hattori, T., Morikawa, K., Kasuga, T., Suzuki, A., Fukui, H. and Niwa, S., 2002, "Development of Low Rigidity β-type Titanium Alloy for Biomedical Applications", Materials Transactions, Vol.43, pp.2970-2977.

Kobayashi, S., Nakagawa, S., Nakai, K. and Ohmori, Y., 2002, "Phase Decomposition ina a Ti-13Nb-13Zr Alloy during Ageing at 600ºC", Materials Transactions, V.43, No.12, pp.2956-2963.

Ramirez, A. J. and Juhas, M. C., 2003, Microstructural Evolution in Ti-6Al-4V Friction Stir Welds, Materials Science Forum, Vol. 426-432, pp. 2999-3004.

Silva, H.M., Schneider, S.G. and Moura Neto, C., 2004, "Study of Nontoxic Aluminum and Vanadium-Free Titanium Alloys for Biomedical Applications", Materials Science & Engineering C, Vol.24, pp. 679-682.

Tang, X., Ahmed, T., Rack, H. J., 2000, "Phase Transformations in Ti-Nb-Ta and Ti-Nb-Ta-Zr Alloys", Journal of Materials Science, Vol.35, pp.1805-1811.

Weiss, I. and Semiatin, S.L., 1998, "Thermomechanical Processing of Beta Titanium Alloys – An Overview" Materials Science and Engineering A, Vol.243, pp. 46-65.

Zhou, Y.L., Niinomi, M. and Akahori, T., 2004, "Decomposition of Martensite α" During Aging Treatments and Resulting Mechanical Properties of Ti-Ta Alloys", Materials Science and Engineering A, Vol. 384, pp.92-101.

5. Responsibility notice

The author(s) is (are) the only responsible for the printed material included in this paper.